PHYS4080 Exoplanet Transit

Ryan White

31st of October 2023

1 Introduction

Ever since the first discovery of an exoplanet via the transit method in 1999 [3], thousands more planets have been found at an increasing rate. The transiting method involves observing dips in apparent brightness of stars as a planet at a near 90° inclined orbit transits across the face of the star from our perspective. With the stellar parameters known (or at least constrained), the depth and duration of the transit allows us to uniquely determine some of the transiting planets physical and orbital characteristics. For example, the depth of the transit is a key constraint on the ratio of the planets radius to the stellar radius. The duration of the transit (together with the depth) describes how fast the planet is moving in its orbit, and hence its orbital parameters overall. Naturally, closely orbiting planets will transit frequently and large planets will have a large transit depth and so this method is biased towards such large planets close to their host stars. Observing the same star for long duration also has the benefit of potentially seeing duplicate transits which helps to reduce error or equivalently find some transits whose transit signal would otherwise be statistically insignificant with only one transit.

One of the most significant surveys in the search for exoplanets is the Wide Angle Search for Planets (WASP) [8]. This survey utilised two wide-field imaging systems at similar longitudes but with one each in the northern and southern hemispheres. The result is effectively multiple surveys of the entire sky each night. Of particular note to us is the star system WASP-44, which was observed to have a planetary companion WASP-44b in 2011 [10]. WASP-44 is a sun-like star, with spectral classification G8V at a distance of ~ 360pc [5], a radius of $0.865R_\odot$ [2, 6], and a mass of $0.917M_\odot$ [6]. The values in the literature suggest that WASP-44b is a transiting hot-Jupiter like planet, orbiting extremely close to the star with a $\sim$ 2.4 day orbit, and a mass and radius comparable to Jupiter [6]. Hence, this planet should have a deep transit of relatively long duration, making it an excellent target for a terrestrial telescope subject to atmospheric distortion and noise.

2 Observing

Available to us was data of the August 7, 2018 transit of WASP-44b observed from the Mount Kent Observatory in Australia. The transit was observed with a Planewave CDK700 0.7m telescope with no filter, allowing all light in to the camera. We see roughly 3 minutes of exposure per frame consistent over the photometric sample, the images captured with a ZWO ASI6200 cooled camera kept at a constant ~ -20°C during the run. Pixels were combined in 4x4 squares to obtain a more consistent signal which was possible due to the reasonably high apparent brightness of WASP-44 in the sky. Data was collected over a duration of ~ 3.6 hours in the early night such that WASP-44 was highest overhead shortly after the end of the transit. The telescope is situated on an Altitude-Azimuthal (Alt-Az) mount, which moves about the two degrees of freedom rotational and inclination. With the fine, precise motors steering the telescope mount, the telescope is able to smoothly track most objects in the sky as the Earth rotates; some difficulty is encountered if the target object is very high in the sky as the mount rotates quickly to maintain tracking while the inclination of the telescope remains relatively constant, often resulting in a quick rotation in the field of view.

In the observation run, bias and dark frames were also captured with the camera. Bias frames are extremely short exposure images with a closed shutter which encode information on the baseline voltage in the CCD [9]. By subtracting these biased frames from our photometry, we effectively remove any effect of a variable voltage baseline in the science images. Similarly, we subtract a series of dark frames which encode the thermal noise in the camera itself. Since the camera effectively stores and records electrons, any thermal fluctuations are going to influence the obtained signal and so this influence is recorded in dark frames which can be corrected for [9].

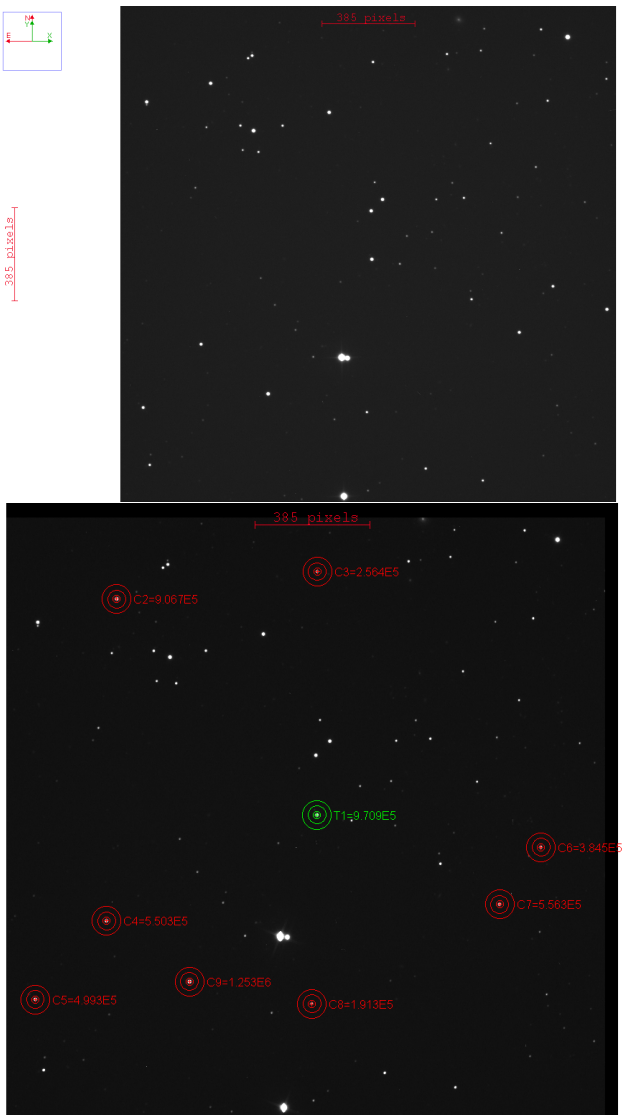

Figure. 1 Our field of view with the telescope, with WASP-44 situated in the center of the image *(top)* with a green annulus in the bottom image and calibration stars shown with red annuli. The brightnesses of the target star and the calibration stars are shown in text next to the annuli, with the resolution scale and orientation in the left of the top image.

3 Analysis and Results

All image processing and modelling was completed with the *AstroImageJ* software [4]. We begin the analysis by subtracting the aforementioned bias and dark frames (9 and 5 frames respectively). Then, we aligned the 62 cleaned frames by selecting a few bright and isolated stars near to the center of the frame and initialising the align stack tool. For this step, we opted to not choose bright stars near to the edge of frame in case they would be cut out of the field of view during the rotation of

Figure. 2 The annulus used in pixel sampling contains the target star within the innermost circle, which forms essentially the raw photometric data of the target. The outermost annulus represents the background pixel values, the median of which is corrected for in the target photometry.

the instrument in the Alt-Az tracking of the target WASP-44. The result was the star field in the frames being constant with respect to movement and rotation and so each star stayed more or less at the same pixels across the photometric sample.

With the alignment complete, we could now turn to light curve and transit modelling within AstroImageJ. The first step was to choose calibration stars for which to compare the brightness of the target star to across the duration of image capturing. Calibration stars were chosen for temporal consistency in their brightness, as well as an order of magnitude similarity in flux to the target star WASP-44. The chosen stars are shown in Figure 1, and are all in the field of view across the entire viewing.

All annuli are to the same configuration as in Figure 2. We chose the radii of the concentric rings small enough to only just capture all pixels of the target and calibration stars, and to capture enough background information without including nearby stars (that may contaminate the background information with intrinsic variability).

With all calibration stars chosen, the timeseries relative flux of the target star was calculated with AstroImageJ. Using multi-aperture differential photometry (by choosing comparison stars) is useful as it allows us to negate or minimise the effects of systematic errors in the data such as camera issues or atmospheric distortion. With this flux calculating, we're able to conveniently use AstroImageJ's transit fitting capability after providing some priors on the stellar and orbital parameters. The transit fitting uses a χ^2 minimisation on several parameters which affect the fit, notably the planetary radius, the semimajor axis of its orbit, the transit center time, the impact parameter of the transit and the limb darkening parameters of the star [4]. We provided order of magnitude estimate priors on the stellar temperature (5400K [2]), the transit center time (on observation of the dip in the data), and the orbital period of the planet (2.43 days [7]) prior to initialising

the transit fitting. The light curve model fit is shown in Figure 3, which we note as an excellent fit to the data with a $\chi^2_{\text{dof}} = 1.02$.
The transit fit gives a range of best-fit values of the planet, albeit with no uncertainty. We obtain a transit depth of 16.57 parts per thousand, which is a key constraint on the planet radius and limb darkening parameters. On this note, we get a squared planet-to-star radius ratio of 0.0149, which, given the star radius in the literature of $0.865R_\odot$ [2], gives a planet radius of $0.1056R_\odot$ or about 1.05 Jupiter radii (agreeing within uncertainty to [1]). As in the legend of Figure 3, we also note the best-fit quadratic limb darkening coefficients for WASP-44 as $u_1 = 0$ and $u_2 = 0.67$. Given the transit duration of approximately 2 hours and 14 minutes and the best fit radius, the orbital semi-major axis of the planet (assuming a circular orbit) was found to be 8.7 stellar radii. Again, given the WASP-44 radius in the literature, this corresponds to a semi-major axis of $a = 7.526R_\odot \simeq 0.035$AU which aligns exactly to the value in the literature to within appropriate significant figures [1]. The model fit also provides a best-fit value on the planetary orbit inclination of 86.7^o in the plane of the sky which aligns within uncertainty to the literature [1].

4 Discussion

On viewing Figure 3, we see that the representative sample of comparison stars (bottom of figure) are relatively consistent in brightness across time. Some of the stars clearly shift upwards or downwards in brightness over time, but these effects cancel out in the multi-aperture differential photometry for our target WASP-44. What we're left with is an excellent timeseries dataset of WASP-44 photometry that has little scatter about the baseline relative brightness of 1. The residual in the model fit is shown above the light curve and we conclude that there are no clear systematic errors in the model fit given by the apparent random scatter in the residuals. We note that as the airmass along the line of sight reduces (given by the increasing trend of the airmass markers in the figure, or see Figure 4), the scatter in the residuals decreases. Intuitively, less air along the line of sight reduces the atmospheric distortion and hence gives us better, more consistent flux data.

As an extra parameter of interest, we tried estimating the mass of WASP-44b using Kepler's third law,

$$\frac{a^3}{T^2} = \frac{G(M+m)}{4\pi^2} \tag{1}$$

although our best fit parameters gave masses for the planet, m, orders of magnitude out of agreement with the literature. We take this error as being due to the weak constraint on the planet orbital period, $T = 2.4$ days, in our fit as equation (1) is extremely sensitive to small changes in the period. Observing multiple consecutive transits and constraining this period would help yield more realistic values for the planetary mass.

Not discussed previously in this report, we originally intended to observe the transit of WASP-147b – another hot-Jupiter like planet. Given the ease of observing these deep hot-Jupiter transits and the frequency at which they occur, these planets are preferentially observed in transit surveys as mentioned earlier. It's interesting to observe these systems that have makeups and dynamics completely unlike our own Solar System which has small, rocky planets orbiting innermost. Although hot-Jupiters can't sustain life in their atmospheres due to their high heat (WASP-44b has a temperature of $\sim$ 1400K [1]), their gravity affects the dynamical stability of any planets in the system including those in the habitable zones which may harbour life. There is also much to be learned about the evaporation of these hot-Jupiter atmospheres (due to their high temperature) and their migration history where these transits and transit surveys provide a unique and cheap (in the context of observing time) method for gathering data at scale.

References

[1] Brett Addison et al. "Minerva-Australis. I. Design, Commissioning, and First Photometric Results". In: *Publications of the Astronomical Society of the Pacific* 131.1005 (Nov. 2019), p. 115003. DOI: 10.1088/1538-3873/ab03aa. arXiv: 1901.11231 [astro-ph.IM].

[2] A. Bonfanti, S. Ortolani, and V. Nascimbeni. "Age consistency between exoplanet hosts and field stars". In: *Astronomy and Astrophysics* 585, A5 (Jan. 2016), A5. DOI: 10.1051/0004-6361/201527297. arXiv: 1511.01744 [astro-ph.SR].

[3] David Charbonneau et al. "Detection of Planetary Transits Across a Sun-like Star". In: *The Astrophysical Journal* 529.1 (Jan. 2000), pp. L45–L48. DOI: 10.1086/312457. arXiv: astro-ph/9911436 [astro-ph].

[4] Karen A. Collins et al. "ASTROIMAGEJ: IMAGE PROCESSING AND PHOTOMETRIC EXTRACTION FOR ULTRA-PRECISE ASTRONOMICAL LIGHT CURVES". In: *The Astronomical Journal* 153.2 (Jan. 2017), p. 77. DOI: 10.3847/1538-3881/153/2/77. URL: https://dx.doi.org/10.3847/1538-3881/153/2/77.

[5] Gaia Collaboration. "VizieR Online Data Catalog: Gaia EDR3 (Gaia Collaboration, 2020)". In: *VizieR Online Data Catalog*, I/350 (Nov. 2020), pp. I/350. DOI: 10.26093/cds/vizier.1350.

[6] L. Mancini et al. “Physical properties of the WASP-44 planetary system from simultaneous multi-colour photometry”. In: *Monthly Notices of the Royal Astronomical Society* 430.4 (Apr. 2013), pp. 2932–2942. DOI: 10.1093/mnras/stt095. arXiv: 1301.3005 [astro-ph.EP].

[7] M. Moyano et al. “Multi-band characterization of the hot Jupiters: WASP-5b, WASP-44b and WASP-46b”. In: *Monthly Notices of the Royal Astronomical Society* 471.1 (Oct. 2017), pp. 650–657. DOI: 10.1093/mnras/stx1612. arXiv: 1708.05700 [astro-ph.EP].

[8] D. L. Pollacco et al. “The WASP Project and the SuperWASP Cameras”. In: *The Publications of the Astronomical Society of the Pacific* 118.848 (Oct. 2006), pp. 1407–1418. DOI: 10.1086/508556. arXiv: astro-ph/0608454 [astro-ph].

[9] Markus Possel. “A Beginner’s Guide to Working with Astronomical Data”. In: *The Open Journal of Astrophysics* 3.1 (Jan. 2020). DOI: 10.21105/astro.1905.13189. URL: https://doi.org/10.21105%2Fastro.1905.13189.

[10] J. T. Wright et al. “The Exoplanet Orbit Database”. In: *The Publications of the Astronomical Society of the Pacific* 123.902 (Apr. 2011), p. 412. DOI: 10.1086/659427. arXiv: 1012.5676 [astro-ph.SR].

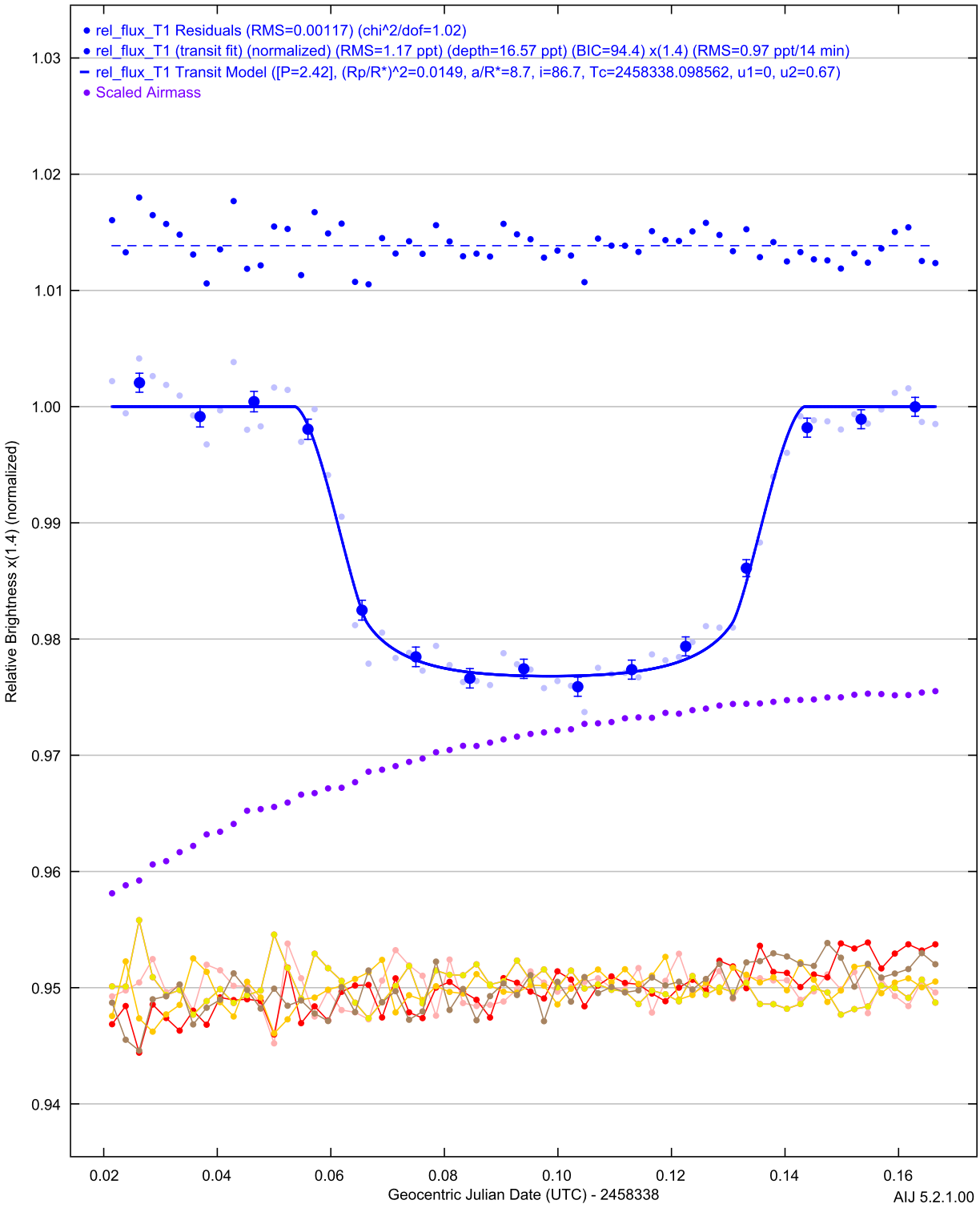

Figure. 3 We present the (scaled) cleaned photometry of WASP-44 with binned averages and a model transit fit in the points around brightness ~ 1.00. For clarity in viewing, only the 8-point binned averages in the data are shown with error. The blue dots scattered about the dashed line at ~ 1.015 brightness shows the residual error in the cleaned photometry with respect to the model fit. The purple dots originating at ~ 0.96 brightness are a qualitative indication of the scaled airmass in front of the field of view, where higher values of these data indicate the target star being higher in the sky and so there is less atmosphere along the line of sight. The data centered around brightness ~ 0.95 is the shifted timeseries brightness of (a representative sample of) calibration stars.

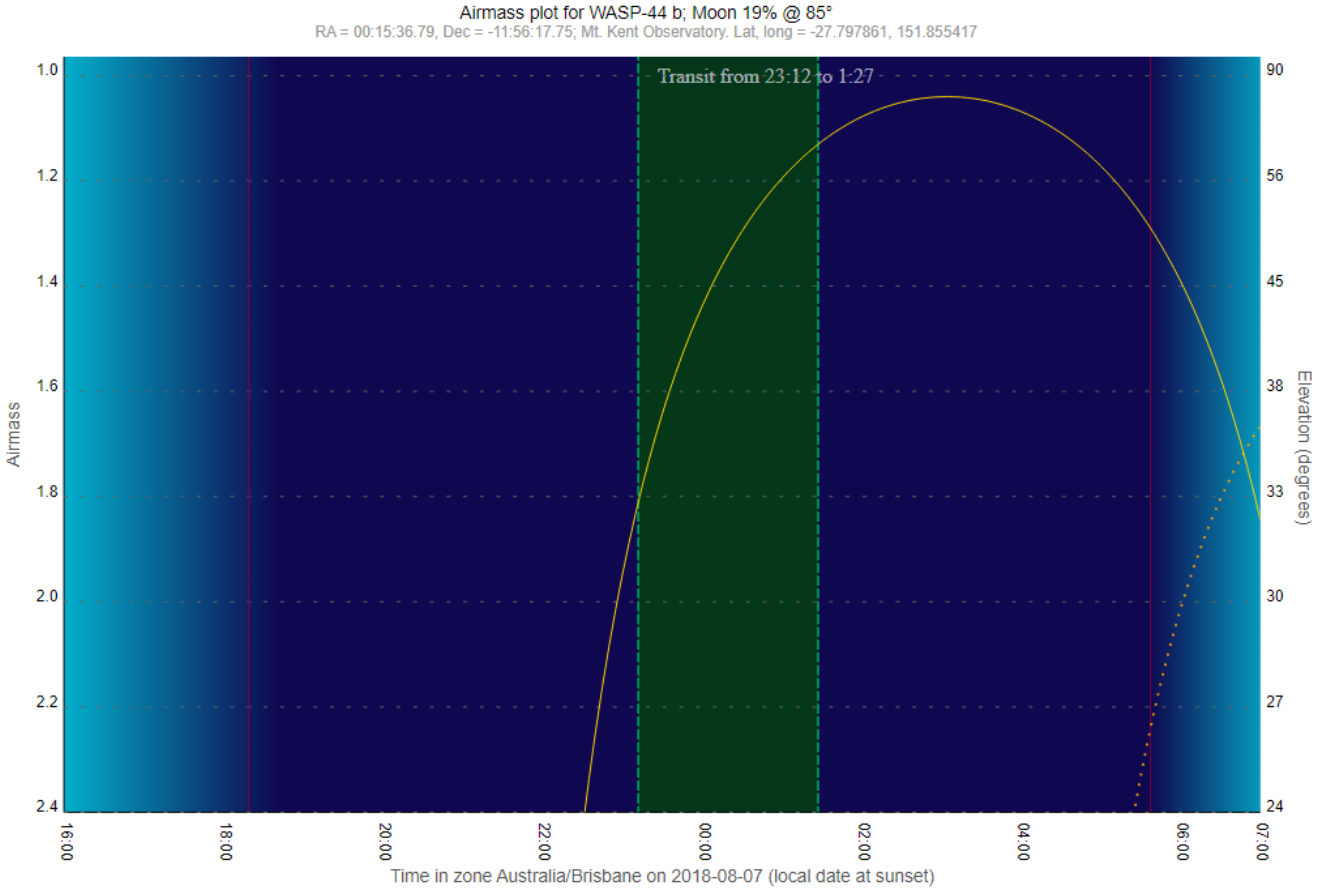

Figure. 4 We see the airmass along the line of sight to WASP-44 go down as the star moves further from the horizon relative to our perspective. The transit duration is almost centered on midnight of August 7, 2018 at the Mount Kent Observatory, with the majority of the transit occurring while the target star is high in the sky.